Control of the molten metal crystallization process in the foundry mold

A. Albu, and V. Zubov

***Abstract*—**The optimal control problem of the metal solidification in casting is considered. The process is modeled by a three-dimensional two-phase initial-boundary value problem of the Stefan type. The mathematical formulation of the optimal control problem for the solidification process is presented. This problem was solved numerically using gradient optimization methods. The gradient of the cost function was computed by applying the fast automatic differentiation technique, which yields the exact value of the cost function gradient for the chosen discrete version of the optimal control problem.

***Keywords*—**Adjoint problem, heat equation, optimal control, Stefan problem.

I. Introduction

THE class of problems in which a material under analysis transforms from one phase into another with heat release or absorption is of great theoretical and practical interest. Such problems arise in studies of many phenomena, among which melting and solidification are the most important and widespread.

The problems arising in practice do not reduce to the description of processes involving phase transitions, but also include control of these processes. Control of processes involving phase transitions is interpreted as the choice of some process parameters (controls) in such a way that the process is as close as possible to a given scenario; for example, the behavior of the liquid-solid phase boundary or a function of temperature in some domain is closest to a required behavior. An effective approach to solving this type of problems was developed and applied in practice by the authors of this article. The efficiency of the method is explained by the *simultaneous* use of three basic elements.

First, during the solution of the initial-boundary value problem that describes the process of heat transfer, the statement of a boundary value problem in terms of temperature is reformulated in terms of enthalpy. The reason for this is the fact that, as one intersects the phase boundary, the temperature changes continuously while the enthalpy undergoes a jump change.

The second element of this approach is a special iterative algorithm proposed by the authors for solving nonlinear systems of finite-difference equations obtained as a result of approximating the initial-boundary value problem. The new iterative algorithm is much more efficient than algorithms used earlier: the modified Jacobi method and the modified Gauss-Seidel method.

Optimal control problems for thermal processes with phase transitions are usually solved numerically using gradient methods. To ensure the efficiency of a gradient method, the gradient of the cost function has to be computed to high accuracy. The third element of the proposed approach is connected with the fact that the gradient of the cost function of the optimal control problem is calculated using the Fast Automatic Differentiation technique ([1]). This method offers canonical formulas that produce the exact value of the gradient in a discrete optimal control problem. In [2] is formulated and substantiated the statement that the time required to find the components of the gradient of the objective function in optimal control problems for thermal processes with phase transitions by this method does not exceed the time of calculating two values of the function.

The problem examined in this article also relates to the problems of control of thermal processes with the phase transitions. For several years the authors of this paper investigated the different aspects of this complex and practically interesting problem.

In [3] a mathematical model of metal solidification in the considered setup was suggested, a finite-difference approximation of the direct problem (of determining the temperature at each point of the object and identifying the solidification front) was proposed, and an algorithm for finding the numerical solution of the direct problem was described. In [4] the choice of a cost functional that models the technological requirements for metal solidification was discussed and optimal control problems for this process were formulated.

In [5] the optimal control of metal solidification was considered in the case where the mold has the simplest shape, namely, a parallelepiped. In [6] and [7] new formulations of the optimal control problem for the solidification process were

This work was supported by the Russian Foundation for Basic Research (project no. 17-07-00493 a) and by the Program "Leading Scientific Schools", no. NSh-8860.2016.1.

Alla Albu is with the Dorodnicyn Computing Centre, FRC CSC RAS, Moscow. Russia (e-mail: alla.albu@mail.ru).

Vladimir Zubov is with the Dorodnicyn Computing Centre, FRC CSC RAS, and Moscow Institute of Physics and Technology, Moscow. Russia (e-mail: vladimir.zubov@mail.ru).

proposed and studied. In [6] were considered three versions of the new model of considered industrial setup in the case of a mold of simplest geometry - a parallelepiped. In [7] the new formulations of the optimal control problem are considered for the case of a mold of complex geometry.

The present work is the final one. Here is represented the complete algorithm, which is based on the indicated above three basic elements, and with the aid of which the problem in question was solved very effectively.

II. Statement of the Problem

The problem under consideration models the solidification of molten metal in casting. It is known that the quality of the resulting casting depends on how the process of cooling and solidification of molten metal proceeds. According to numerous studies of this process, for a product of high quality to be obtained, it is desirable the shape of the phase boundary to be as close to a plane as possible and its speed to be close to a prescribed one.

Fig. 1 represents the longitudinal projections of an actual mold, which is filled with liquid metal. The mold and the metal inside it are heated up to prescribed temperatures T_{form} and T_{met}, respectively. Next, the object (the mold and the metal inside it) begins to cool gradually under varying external conditions.

The solidification process is controlled using a special industrial setup, which consists of upper and lower parts. The upper part is a furnace with the object moving inside it. It is modeled by two vertical parallel walls joined above by a horizontal wall ("ceiling"). The walls and ceiling of the furnace are heated up to a prescribed rather high temperature. The lower part of the setup is a coolant representing a large tank filled with liquid aluminum whose temperature is somewhat higher than the aluminum melting point (about 1000°K degrees). In this work we consider a version in which two lateral walls of the mold (on the sides where there are no furnace walls) are heat-insulated. This model also describes the situation when several molds are lined up in the furnace and are located near from each other.

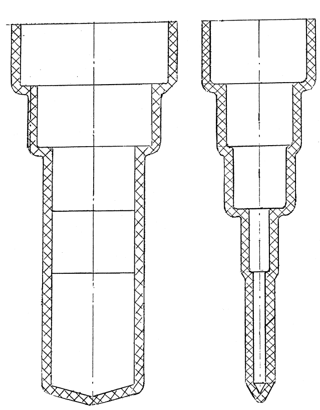

Fig. 1. Schematic view of the mold (two projections).

The metal-filled mold is slowly immersed in the coolant. The liquid aluminum has a relatively low temperature, which causes the solidification of the metal. However, the object gains heat from the furnace walls, which prevents the solidification process from proceeding too fast. The problem is to choose a regime of metal cooling and solidification (such control parameters) at which the solidification front has a preset shape and moves at a speed close to the preset one.

The computational domain of the problem (domain Q) is the area of the mold and the metal inside it, Γ is a piecewise-smooth boundary of Q. The cooling of the metal and the mold is governed by the three-dimensional non-stationary heat equation:

$$\frac{\partial H}{\partial t} = \frac{\partial}{\partial x}\left(K\frac{\partial T}{\partial x}\right) + \frac{\partial}{\partial y}\left(K\frac{\partial T}{\partial y}\right) + \frac{\partial}{\partial z}\left(K\frac{\partial T}{\partial z}\right),$$
$$(x,y,z) \in Q.$$

Here, T is the temperature of the substance at the point with coordinates (x,y,z) at time t.

The thermal conductivity has the form:

$$K(T) = \begin{cases} K_1(T), & (x,y,z) \in metal, \\ K_2(T), & (x,y,z) \in mold, \end{cases}$$

$$K_1(T) = \begin{cases} k_S, & T < T_1, \\ \dfrac{k_L - k_S}{T_2 - T_1} T + \dfrac{k_S T_2 - k_L T_1}{T_2 - T_1}, & T_1 \le T < T_2, \\ k_L, & T \ge T_2, \end{cases}$$

$$K_2(T) = \begin{cases} k_{\Phi_1}, & T \le T_3, \\ k_{\Phi_2}, & T_3 < T. \end{cases}$$

The heat content function $H(T(x,y,z,t))$ is defined as

$$H(T(x,y,z,t)) = \begin{cases} H_1(T), & (x,y,z) \in metal, \\ H_2(T), & (x,y,z) \in mold, \end{cases}$$

$$H_1(T) = \begin{cases} \rho_S c_S T, & T < T_1, \\ \dfrac{\rho_S c_S (T_2 - T_1) + \rho_S \gamma}{T_2 - T_1} T - \dfrac{\rho_S \gamma T_1}{T_2 - T_1}, & T_1 \le T < T_2, \\ \rho_L c_L (T - T_2) + \rho_S c_S T_2 + \rho_S \gamma, & T \ge T_2, \end{cases}$$

$$H_2(T) = \rho_\Phi c_\Phi T,$$

where γ is the specific heat of melting.

Here, c_S, c_L, c_Φ, ρ_S, ρ_L, ρ_Φ, k_S, k_L, k_Φ, T_1, T_2, and T_3 are prescribed constants (the indices L and S denote the liquid and solid phases, respectively). The thermodynamic coefficients (the density of the substance, the heat capacity, and thermal conductivity) have a jump at the metal–mold interface. Two conditions are required to hold at this surface; namely, the temperature and the heat flux must be continuous. The metal can be simultaneously in two phases: solid and liquid. The domain separating the phases is determined by the narrow range of temperatures $[T_1, T_2]$, in which the thermodynamic coefficients and the content function vary rapidly.

A distinctive feature of this problem is that the substance under study undergoes phase transitions (from liquid to solid states and back) accompanied by heat release or absorption (Stefan-type problems). The law of motion of the phase boundary is not known beforehand and has to be determined.

All the heat exchange conditions on the boundary Γ of Q can be written in the general form $\alpha T + \beta T_{\boldsymbol{n}} = \varphi$. Here, α, β and φ are given functions of the coordinates (x, y, z) of a point on Γ and of the temperature T, while $T_{\boldsymbol{n}}$ is the derivative of the temperature T in the outward normal direction $\boldsymbol{n}$ to Γ.

The cooling of the mold and the metal inside it occurs due to the interaction of the object with its surroundings. It is important to note that the different parts of its outer boundary are under different thermal conditions (i.e., the laws of heat transfer with the surroundings are different in these parts). Moreover, the parts themselves and the thermal conditions affecting them vary with time.

If the point is in the molten aluminum, then in this case it is necessary to take into account:

1) the heat lost by the body due to its own radiation;
2) the heat gained from the surrounding liquid aluminum;
3) the heat transfer due to conduction between the liquid aluminum and the body.

If the point is outside the molten aluminum, then in this case it is necessary to take into account:

1) the heat lost by the body due to its own radiation;
2) the heat gained from the emitting walls of the furnace;
3) the heat gained from the emitting surface of the liquid aluminum;
4) the heat gained from the emitting surface of roof.

One of the basic mechanisms of heat transfer in this problem is thermal radiation. To determine the heat flux coming to the surface of the object from hot surfaces, it is necessary to solve a rather complicated boundary-value problem. In [8] a mathematical model of heat transfer process due to radiation from the heated surface to the mold is proposed. During the simulation of this process the special features of the considered experimental setup were taken into account. An algorithm for calculating the heat flux based on the constructed model was proposed. It is based on the final formula, obtained from the integration of general relations, which describe the propagation of thermal radiation.

The evolution of the phase boundary is affected by many parameters (for example, the furnace temperature, the temperature of the liquid aluminum, the depth to which the object is immersed in the liquid aluminum, the velocity of the object relative to the furnace, etc.). Of special interest in practice is the dependence of the phase boundary on the velocity of the object moving in the furnace. For this reason, as a control function we use the velocity of the mold in the furnace. If we do not control the speed of the motion of the object, then "bubbles" of liquid metal form and collapse inside the casting during the process of crystallization, which results in a casting of poor quality.

To find a control function satisfying the technological requirements, we formulate an optimal control problem for metal solidification. This problem consists of choosing a mode of metal cooling and solidification in which the solidification front has a preset shape (it is desirable the front to be a plane orthogonal to the vertical axis of the object) and moves at a speed close to the preset one.

The velocity of the mold relative to the furnace (control function) is determined by solving the following optimal control problem. We introduce two classes of functions: $\tilde{K}_1$ and $\tilde{K}_2$. Let A_* and B_* be a priori given constants (more specifically, A_* is the z-coordinate determining the initial position of the object relative to the furnace and B_* is the z-coordinate determining the position of the object relative to the furnace at the maximum depth to which the object is immersed in the coolant). A function $\tilde{u}(t)$ is said to belong to the class $\tilde{K}_1$ if $\tilde{u}(t)$ is continuous and piecewise smooth for $t \in [0, \infty)$ and satisfies the constraints $A_* \le \tilde{u}(t) \le B_*$ and $\tilde{u}(0) = A_*$. The class $\tilde{K}_2$ consists of all piecewise continuous functions $u(t)$, $t \in [0, \infty)$, that are obtained by differentiating functions from $\tilde{K}_1$. A valid control will be a function of class $\tilde{K}_2$.

A major element of any optimal control problem is the cost functional. The studies dedicated to the choice of a functional satisfying the technological requirements for the process of metal solidification are carried out. The basic cost functional is defined as:

$$I(u) = \frac{1}{t_2(u) - t_1(u)} \int_{t_1(u)}^{t_2(u)} \iint_S \left[Z_{pl}(x, y, t) - z_*(t)\right]^2 dx dy\, dt .$$

Here t_1 is the time at which the solidification front is initially formed, t_2 is the time at which the metal becomes completely solid, $S = S(t)$ is the projection of the phase boundary onto a plane perpendicular to the vertical axis of the mold, $\left(x, y, Z_{pl}(x, y, t)\right)$ are the actual coordinates of points on the phase boundary at the time *t*, and $\left(x, y, z_*(t)\right)$ are the desired coordinates of points on the phase boundary at the time *t*. The coordinates of the phase boundary are determined from the following equation: $T(x, y, Z_{pl}(x, y, t, u(t)), t) = T_{pl}$, where T_{pl} is the temperature of the solidification of metal, which is equal to $T_{pl} = (T_1 + T_2)/2$.

Functional $I(u)$ is the time-average rms deviation of the actual phase boundary from the desired one. It is designed to ensure that the front velocity is close to the desired one and provides the flattening of this surface. The optimal control problem is to determine a control $u(t) \in \tilde{K}_2$ that minimizes the cost functional.

III. Algorithm for Determining the Temperature Field of the Object

The first element of the solution of the optimal control problem is the direct problem (finding the temperature at each point and determining the solidification front). The numerical algorithm for solving the direct problem is based on the heat balance equation. Additionally, we proceed from the problem formulation in terms of temperature to that in terms of heat content.

The object under study is approximated by a body consisting of a finite number of parallelepipeds. This body is mentally placed in an auxiliary parallelepiped whose sizes coincide with those of the object.

We introduce a coordinate system tied to the moving mold. The Oz axis is directed vertically upward, the Ox axis lies in a horizontal plane and is directed from left to right, and the Oy axis is chosen so that $Oxyz$ is a right-hand coordinate system. The origin O is placed at the front bottom left vertex of the auxiliary parallelepiped.

The time grid is defined by introducing grid nodes $\{t^j\}$, $j=\overline{0,J}$, with the steps $\tau^j = t^j - t^{j-1}$, $j=\overline{1,J}$. We also introduce two spatial grids (generally non-uniform): the basic grid $\{x_n\}$, $n=\overline{0,N}$; $\{y_i\}$, $i=\overline{0,I}$; $\{z_l\}$, $l=\overline{0,L}$; with the mesh sizes:

$$h_n^x = x_{n+1} - x_n,\ n=\overline{0,N-1};\quad h_i^y = y_{i+1} - y_i,\ i=\overline{0,I-1};$$

$$h_l^z = z_{l+1} - z_l,\ l=\overline{0,L-1};$$

and the auxiliary grid

$$\tilde{x}_0 = x_0;\quad \tilde{x}_n = x_{n-1} + h_{n-1}^x/2;\quad n=\overline{1,N};\quad \tilde{x}_{N+1} = x_N;$$

$$\tilde{y}_0 = y_0;\quad \tilde{y}_i = y_{i-1} + h_{i-1}^y/2;\quad i=\overline{1,I};\quad \tilde{y}_{I+1} = y_I;$$

$$\tilde{z}_0 = z_0;\quad \tilde{z}_l = z_{l-1} + h_{l-1}^z/2;\quad l=\overline{1,L};\quad \tilde{z}_{L+1} = z_L.$$

The basic grid is constructed so that all the outer surfaces of the approximating body and all the metal-mold interfaces are coordinate surfaces of this grid. Note that each of M parallelepipeds that comprise the object contains points (x_n, y_i, z_l) of the basic grid for which $n^*(m) \le n \le N^*(m)$, $i^*(m) \le i \le I^*(m)$, $l^*(m) \le l \le L^*(m)$, $m=\overline{1,M}$. (For the object shown in Fig. 1, $M=5$.)

The surfaces of the auxiliary grid are parallel to those of the basic grid, while the nodes of the former lie at the midpoints of the segments joining the nodes of the latter. The planes $x=\tilde{x}_n$, $y=\tilde{y}_i$, and $z=\tilde{z}_l$ divide the object into elementary cells. An elementary cell is assigned the indices (n,i,l) if the cell vertex nearest to the origin coincides with the grid point $(\tilde{x}_n, \tilde{y}_i, \tilde{z}_l)$. The volume of such an elementary cell is denoted by V_{nil} and its outer surface by S_{nil}. Let's denote the average temperature in the cell as $T_{nil}(t)$.

Any elementary cell is either completely filled with a single medium (metal or mold) or some part of it is filled with one medium and the remaining part with the other. Let V_{nil}^1 denote the part of V_{nil} filled with metal and V_{nil}^2 denote the part of V_{nil} filled with the mold material. Similarly, S_{nil}^1 is the part of S_{nil} that is adjacent to V_{nil}^1 and S_{nil}^2 is the part of S_{nil} that is adjacent to V_{nil}^2.

If the object is a parallelepiped, all the elementary cells are also parallelepipeds (Fig. 2a). If the object is of complex geometry, then, at the interfaces of different parts of the object, there arise new elementary cells of complex shape that were not encountered earlier. They have the form shown in Fig. 2b,c. Such cells always have faces on the outer boundary of the mold. As a result, the configuration of S_{nil}^2 becomes more complex. The complex configuration of the cells must be considered when determining heat fluxes in such cells.

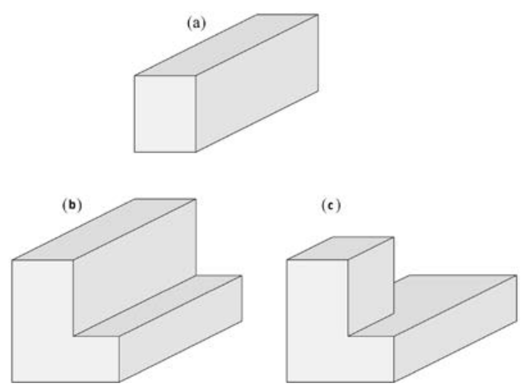

Fig. 2 Forms of computational cells

The numerical solution of the direct problem is based on the heat balance equation. For the cell indexed by (n,i,l), this equation has the form

$$\iiint_{V_{nil}^1} \left[H_1\left(T_{nil}^{j+1}\right) - H_1\left(T_{nil}^{j}\right)\right] dV + \iiint_{V_{nil}^2} \left[H_2\left(T_{nil}^{j+1}\right) - H_2\left(T_{nil}^{j}\right)\right] dV =$$

$$= \int_{t^j}^{t^{j+1}} \left[\iint_{S_{nil}^1} K_1\left(\tilde{T}_{nil}(t)\right)\left(\tilde{T}_{\boldsymbol{n}}(t)\right)_{nil} ds + \iint_{S_{nil}^2} K_2\left(\tilde{T}_{nil}(t)\right)\left(\tilde{T}_{\boldsymbol{n}}(t)\right)_{nil} ds \right] dt \cdot$$

Here, $T_{nil}^j = T_{nil}\left(t^j\right)$, while $K_1\left(\tilde{T}_{nil}(t)\right) \cdot \left(\tilde{T}_{\boldsymbol{n}}(t)\right)_{nil}$ and

$K_2(\tilde{T}_{nil}(t))\cdot(\tilde{T}_{\mathbf{n}}(t))_{nil}$ are the heat flux densities through the cell surface for the metal and the mold, respectively. Integration of the left part of last equality gives

$$\left[V_{nil}^1 H_1\left(T_{nil}^{j+1}\right)+V_{nil}^2 H_2\left(T_{nil}^{j+1}\right)\right]- \\ -\left[V_{nil}^1 H_1\left(T_{nil}^{j}\right)+V_{nil}^2 H_2\left(T_{nil}^{j}\right)\right]= \\ =\int_{t^j}^{t^{j+1}}\left[\iint_{S_{nil}^1} K_1\left(\tilde{T}_{nil}(t)\right)\cdot\left(\tilde{T}_{\mathbf{n}}(t)\right)_{nil} ds\right]dt+ \\ +\int_{t^j}^{t^{j+1}}\left[\iint_{S_{nil}^2} K_2\left(\tilde{T}_{nil}(t)\right)\cdot\left(\tilde{T}_{\mathbf{n}}(t)\right)_{nil} ds\right]dt. \qquad (1)$$

Next, the formulation of the boundary value problem in terms of temperature is reformulated in terms of enthalpy. The considered computational domain is inhomogeneous (contains metal and the material of the form). In order to better take into account the geometry of cells, and how they are filled, the concept of the so-called "total density of heat content" in the cell is introduced. Let $M_{nil}=V_{nil}^1/V_{nil}$ be the volume fraction of the metal in the elementary cell indexed by (n,i,l), and let $\Phi_{nil}=V_{nil}^2/V_{nil}$ be the volume fraction of the mold in this cell. Denote by $E_{nil}^j=M_{nil}H_1\left(T_{nil}^j\right)+\Phi_{nil}H_2\left(T_{nil}^j\right)$ the total heat content density in the cell (n,i,l) at the time t^j. Taking into account the relations defining $H_1(T)$ and $H_2(T)$, we obtain an expression for $E_{nil}^j(T_{nil}^j)$:

$$E_{nil}^j\left(T_{nil}^j\right)=\begin{cases} a_{nil}T_{nil}^j, & T_{nil}^j<T_1, \\ b_{nil}^1 T_{nil}^j-b_{nil}^2, & T_1\le T_{nil}^j<T_2, \\ d_{nil}^1 T_{nil}^j+d_{nil}^2, & T_{nil}^j\ge T_2, \end{cases}$$

where
$$a_{nil}=M_{nil}\rho_S c_S+\Phi_{nil}\rho_\Phi c_\Phi,$$
$$b_{nil}^1=M_{nil}\left(\rho_S c_S+\rho_S\lambda/(T_2-T)\right)+\Phi_{nil}\rho_\Phi c_\Phi,$$
$$b_{nil}^2=M_{nil}\rho_S\lambda T_1/\left(T_2-T_1\right),$$
$$d_{nil}^1=M_{nil}\rho_L c_L+\Phi_{nil}\rho_\Phi c_\Phi,$$
$$d_{nil}^2=M_{nil}\cdot\left(\rho_S\lambda+(\rho_S c_S-\rho_L c_L)\cdot T_2\right).$$

The temperature T_{nil}^j is defined as the inverse of $E_{nil}^j(T_{nil}^j)$:

$$T_{nil}^j\equiv\beta\left(E_{nil}^j\right)=\begin{cases} \dfrac{E_{nil}^j}{a_{nil}}, & E_{nil}^j<a_{nil}T_1, \\ \dfrac{E_{nil}^j+b_{nil}^2}{b_{nil}^1}, & a_{nil}T_1\le E_{nil}^j<d_{nil}^1T_2+d_{nil}^2, \\ \dfrac{E_{nil}^j-d_{nil}^2}{d_{nil}^1}, & E_{nil}^j\ge d_{nil}^1T_2+d_{nil}^2. \end{cases}$$

The functions $K_1\left(T_{nil}^j\right)$ and $K_2\left(T_{nil}^j\right)$ can also be expressed in terms of E_{nil}^j:

$$K_1\left(T_{nil}^j\right)\equiv\Omega_1\left(E_{nil}^j\right)= \\ =\begin{cases} k_S, & E_{nil}^j<E_1, \\ \dfrac{k_L-k_S}{E_2-E_1}E_{nil}^j+\dfrac{k_SE_2-k_LE_1}{E_2-E_1}, & E_1\le E_{nil}^j<E_2, \\ k_L, & E_{nil}^j\ge E_2, \end{cases}$$

$$K_2\left(T_{nil}^j\right)\equiv\Omega_2\left(E_{nil}^j\right)= \\ =\begin{cases} k_{\Phi_1}, & E_{nil}^j<E_3, \\ \dfrac{k_{\Phi_2}-k_{\Phi_1}}{E_4-E_3}E_{nil}^j+\dfrac{k_{\Phi_1}E_4-k_{\Phi_2}E_3}{E_4-E_3}, & E_3\le E_{nil}^j<E_4, \\ k_{\Phi_2}, & E_{nil}^j\ge E_4, \end{cases}$$

$$E_1\equiv\rho_S c_S T_1, \qquad E_2\equiv\rho_S\left(c_S T_2+\gamma\right),$$
$$E_3\equiv\rho_\Phi c_\Phi\left(T_3-\delta\right), E_4\equiv\rho_\Phi c_\Phi\left(T_3+\delta\right), \quad \delta<<T_3.$$

Function $E_{nil}^j(T_{nil}^j)$ as a function that depends on the temperature in the metal behaves as a function $H_1(T)$, i.e. in a narrow temperature range $[T_1,T_2]$ is changing very quickly, almost abruptly. For this reason, iterative methods for solving systems of equations that approximate the heat balance equation converge poorly.

The temperature T_{nil}^j as a function that depends on the total density of heat content does not change so quickly, and when the specified conditions are satisfied, the algorithms for solving the direct problem are guaranteed to converge. Taking into account this fact, in the equality (1) let us pass from the variable $T_{nil}(t)$ to the variable $E_{nil}(t)$:

$$V_{nil}\cdot\left(E_{nil}^{j+1}-E_{nil}^j\right)= \\ =\int_{t^j}^{t^{j+1}}\left[\iint_{S_{nil}^1}A_1\left(E_{nil}(t)\right)ds+\iint_{S_{nil}^2}A_2\left(E_{nil}(t)\right)ds\right]dt, \qquad (2)$$

where
$$A_1\left(E_{nil}(t)\right)=\Omega_1\left(\tilde{E}_{nil}(t)\right)\cdot\beta_{\mathbf{n}}\left(\tilde{E}_{nil}(t)\right),$$
$$A_2\left(E_{nil}(t)\right)=\Omega_2\left(\tilde{E}_{nil}(t)\right)\cdot\beta_{\mathbf{n}}\left(\tilde{E}_{nil}(t)\right),$$

$$\left(\begin{array}{l} j=\overline{0,J-1};\ n=\overline{n^*(m),N^*(m)};\ i=\overline{i^*(m),I^*(m)}; \\ l=\overline{l^*(m),L^*(m)};\ m=\overline{1,M} \end{array}\right).$$

Equation (2) is the heat balance equation, written in terms of enthalpy function for any cell of the object being investigated.

Equation (2) is discretized in time using the Peaceman–Rachford scheme, two-layer implicit scheme with weights, and a locally one-dimensional scheme ([9], [10]). The results produced by the three difference schemes were compared with each other.

The locally one-dimensional scheme performs with a large time step (thus saving CPU time) and is easy to implement, but is considerably inferior to the other schemes in terms of accuracy. Solution using an implicit scheme with weights seem physically more justified. A large number of calculations of the direct problem was carried out at a sufficiently wide range of input data (the furnace temperature, the temperature of the liquid aluminum, the depth to which the object is immersed in the liquid aluminum, the velocity of the object relative to the furnace). All calculations have shown that the use of the Peaceman–Rachford scheme gives the same accuracy of the solution of the direct problem as the two-layer implicit scheme with weights, but with the aid of the Peaceman–Rachford scheme the direct problem is solved considerably faster (see [4]). This scheme has a sufficiently large time step and requires much less CPU time than the implicit scheme with weights. The Peaceman–Rachford scheme was used to solve the optimal control problem.

We introduce the following notation, which is used to write the time discretization of (2) in a more compact form:

$$\tilde{\Lambda}_x E = \iint\limits_{S_{nil}^{1x+} \cup S_{nil}^{1x-}} A_1(E)ds + \iint\limits_{S_{nil}^{2x+} \cup S_{nil}^{2x-}} A_2(E)ds + \iint\limits_{S_{nil}^{2xd}} A_2(E)ds,$$

$$\tilde{\Lambda}_y E = \iint\limits_{S_{nil}^{1y+} \cup S_{nil}^{1y-}} A_1(E)ds + \iint\limits_{S_{nil}^{2y+} \cup S_{nil}^{2y-}} A_2(E)ds + \iint\limits_{S_{nil}^{2yd}} A_2(E)ds,$$

$$\tilde{\Lambda}_z E = \iint\limits_{S_{nil}^{1z+} \cup S_{nil}^{1z-}} A_1(E)ds + \iint\limits_{S_{nil}^{2z+} \cup S_{nil}^{2z-}} A_2(E)ds + \iint\limits_{S_{nil}^{2zd}} A_2(E)ds \cdot$$

Here, S_{nil}^{1x+} denotes the part of S_{nil}^{1} that belongs to the plane $x = \tilde{x}_{n+1}$, while S_{nil}^{1x-} denotes the part of S_{nil}^{1} that belongs to the plane $x = \tilde{x}_n$. The surfaces $S_{nil}^{1y+}, \ldots, S_{nil}^{1z-}$, and $S_{nil}^{2x+}, \ldots, S_{nil}^{2z-}$, are defined in a similar manner. The surfaces S_{nil}^{2xd}, S_{nil}^{2yd} and S_{nil}^{2zd} are additional ones occurring in cells of complex geometry. For example, S_{nil}^{2xd} is the part of S_{nil}^{2} that belongs to the plane $x = x_n$. When some or all additional surfaces are absent (in the latter case, the cell has the shape of a box), their surface areas are set equal to zero.

The time discretization of (2) based on the Peaceman–Rachford scheme has the form:

$$V_{nil} \cdot \left(E_{nil}^{j+1} - E_{nil}^{j}\right) = \frac{2\tau}{3}\tilde{\Lambda}_x E_{nil}^{j+1/3} + \frac{\tau}{3}\tilde{\Lambda}_x E_{nil}^{j+2/3} + \frac{\tau}{3}\tilde{\Lambda}_y E_{nil}^{j} + \frac{2\tau}{3}\tilde{\Lambda}_y E_{nil}^{j+2/3} + \frac{\tau}{3}\tilde{\Lambda}_z E_{nil}^{j} + \frac{\tau}{3}\tilde{\Lambda}_z E_{nil}^{j+1/3} + \frac{\tau}{3}\tilde{\Lambda}_z E_{nil}^{j+1}, \quad (3)$$

$$\left(\begin{array}{l} j = \overline{0, J-1};\ n = \overline{n^*(m), N^*(m)};\ i = \overline{i^*(m), I^*(m)}; \\ l = \overline{l^*(m), L^*(m)};\ m = \overline{1, M} \end{array} \right).$$

Here,

$$E_{nil}^{j+1/3} = E_{nil}\left(t^j + \tau/3\right), \qquad E_{nil}^{j+2/3} = E_{nil}\left(t^j + 2\tau/3\right).$$

The values $V_{nil}E_{nil}^{j+1/3}$ and $V_{nil}E_{nil}^{j+2/3}$ are added to and subtracted from the left-hand side of (3) and the result is divided into three equations (with splitting into the x, y and z directions) to obtain the following three subproblems:

x-direction:

$$V_{nil} \cdot \left(E_{nil}^{j+1/3} - E_{nil}^{j}\right) = \frac{\tau}{3}\tilde{\Lambda}_x E_{nil}^{j+1/3} + \frac{\tau}{3}\tilde{\Lambda}_y E_{nil}^{j} + \frac{\tau}{3}\tilde{\Lambda}_z E_{nil}^{j},$$

y-direction:

$$V_{nil} \cdot \left(E_{nil}^{j+2/3} - E_{nil}^{j+1/3}\right) = \frac{\tau}{3}\tilde{\Lambda}_y E_{nil}^{j+2/3} + \frac{\tau}{3}\tilde{\Lambda}_x E_{nil}^{j+1/3} + \frac{\tau}{3}\tilde{\Lambda}_z E_{nil}^{j+1/3},$$

z-direction:

$$V_{nil} \cdot \left(E_{nil}^{j+1} - E_{nil}^{j+2/3}\right) = \frac{\tau}{3}\tilde{\Lambda}_z E_{nil}^{j+1} + \frac{\tau}{3}\tilde{\Lambda}_x E_{nil}^{j+2/3} + \frac{\tau}{3}\tilde{\Lambda}_y E_{nil}^{j+2/3},$$

$$\left(\begin{array}{l} j = \overline{0, J-1};\ n = \overline{n^*(m), N^*(m)};\ i = \overline{i^*(m), I^*(m)}; \\ l = \overline{l^*(m), L^*(m)};\ m = \overline{1, M} \end{array} \right).$$

The thermal conductivities $\Omega_1\left(\tilde{E}_{nil}^{j}\right)$ and $\Omega_2\left(\tilde{E}_{nil}^{j}\right)$ on the internal surfaces of an elementary cell are approximated in the usual manner. For example,

$$\Omega_1\left(\tilde{E}_{nil}^{j}\right)\Big|_{S_{nil}^{1x+}} = \frac{\Omega_1\left(E_{nil}^{j}\right) + \Omega_1\left(E_{n+1,il}^{j}\right)}{2} \equiv R_n^j,$$

$$\Omega_1\left(\tilde{E}_{nil}^{j}\right)\Big|_{S_{nil}^{1x-}} = \frac{\Omega_1\left(E_{n-1,il}^{j}\right) + \Omega_1\left(E_{nil}^{j}\right)}{2} \equiv R_{n-1}^j,$$

$$\Omega_1\left(\tilde{E}_{nil}^{j}\right)\Big|_{S_{nil}^{1y+}} = \frac{\Omega_1\left(E_{nil}^{j}\right) + \Omega_1\left(E_{n,i+1,l}^{j}\right)}{2} \equiv \hat{R}_i^j,$$

$$\Omega_1\left(\tilde{E}_{nil}^{j}\right)\Big|_{S_{nil}^{1y-}} = \frac{\Omega_1\left(E_{nil}^{j}\right) + \Omega_1\left(E_{n,i-1,l}^{j}\right)}{2} \equiv \hat{R}_{i-1}^j.$$

The notation $\tilde{R}_l^j$ and $\tilde{R}_{l-1}^j$ for the surfaces S_{nil}^{1z+} and S_{nil}^{1z-} and similar notation for $\Omega_2\left(\tilde{E}_{nil}^{j}\right)$, namely, B_n^j, B_{n-1}^j, $\hat{B}_i^j$, $\hat{B}_{i-1}^j$, $\tilde{B}_l^j$, and $\tilde{B}_{l-1}^j$ are introduced in a similar manner.

Boundary conditions $\alpha T + \beta T_{\boldsymbol{n}} = \varphi$ on the outer boundary Γ of the object can be rewritten in the general form

$$K(T)T_{\boldsymbol{n}}\big|_{\Gamma} = \left(r(T)T + q(t)\right)\big|_{\Gamma}.$$

Since

$$K(T) = \begin{cases} K_1(T), & (x,y,z) \in S_{nil}^{1} \\ K_2(T), & (x,y,z) \in S_{nil}^{2} \end{cases} = \begin{cases} \Omega_1(E), & (x,y,z) \in S_{nil}^{1}, \\ \Omega_2(E), & (x,y,z) \in S_{nil}^{2}, \end{cases}$$

the last expression splits into two:

$$\Omega_1(E)\beta_{\boldsymbol{n}}(E)\big|_{\Gamma} = \left(r_1(\beta(E))\beta(E) + q_1(t)\right)\big|_{\Gamma},\ (x,y,z) \in S_{nil}^{1},$$

$$\Omega_2(E)\beta_{\boldsymbol{n}}(E)\big|_{\Gamma} = \left(r_2(\beta(E))\beta(E) + q_2(t)\right)\big|_{\Gamma}, \ (x,y,z) \in S_{nil}^2 .$$

In [11] these two boundary conditions were described in detail and expressions for $r_1(\beta(E))$, $q_1(t)$, $r_2(\beta(E))$, and $q_2(t)$ were derived.

In the above three subproblems, the outward normal derivatives $\beta_{\boldsymbol{n}}(E)$ are approximated by the formula $\beta_{\boldsymbol{n}}(E) = (\nabla \beta, \boldsymbol{n})$. For example,

$$\beta_{\boldsymbol{n}}(\tilde{E}_{nil}^{j})\Big|_{S_{nil}^{2x+}} = \frac{\beta_{n+1,il}^{j} - \beta_{nil}^{j}}{h_n^x}, \qquad n = \overline{n^*(m), N^*(m)-1},$$

$$\beta_{\boldsymbol{n}}(\tilde{E}_{nil}^{j})\Big|_{S_{nil}^{2x-}} = -\frac{\beta_{nil}^{j} - \beta_{n-1,il}^{j}}{h_{n-1}^x}, \qquad n = \overline{n^*(m)+1, N^*(m)} .$$

where $\beta_{nil}^j = \beta\left(E_{nil}^j\right)$.

We also introduce the function $L^{**}(n,i)$ defined as the number of cells of the object with the first index equal to n and the second index equal to i.

Since the object is symmetric about the vertical axis and is located symmetrically about the furnace centerline, for simplicity, the algorithm is described for a quarter of the object. For $n = 0$ and $i = 0$, the symmetry conditions are used as boundary conditions.

With the notation introduced, the spatial approximation of the first subproblem inside the domain under consideration can be written as

$$E_{nil}^{j+\frac{1}{3}} - E_{nil}^{j} = w_{nil}^{j+1}\Bigg[S_{nil}^{1x+} R_n^{j+1/3} \frac{\beta_{n+1,il}^{j+\frac{1}{3}} - \beta_{nil}^{j+\frac{1}{3}}}{h_n^x} -$$

$$- S_{nil}^{1x-} R_{n-1}^{j+\frac{1}{3}} \frac{\beta_{nil}^{j+\frac{1}{3}} - \beta_{n-1,il}^{j+\frac{1}{3}}}{h_{n-1}^x} + S_{nil}^{2x+} B_n^{j+\frac{1}{3}} \frac{\beta_{n+1,il}^{j+\frac{1}{3}} - \beta_{nil}^{j+\frac{1}{3}}}{h_n^x} -$$

$$- S_{nil}^{2x-} B_{n-1}^{j+\frac{1}{3}} \frac{\beta_{nil}^{j+\frac{1}{3}} - \beta_{n-1,il}^{j+\frac{1}{3}}}{h_{n-1}^x} +$$

$$+ S_{nil}^{2xd} \left(r_2\left(\beta_{nil}^{j+\frac{1}{3}} \right) \beta_{nil}^{j+\frac{1}{3}} + q_2^{j+\frac{1}{3}} \right)\Big|_{S_{nil}^{2xd}} \Bigg] +$$

$$+ w_{nil}^{j+1}\Bigg[S_{nil}^{1y+} \hat{R}_i^j \frac{\beta_{n,i+1,l}^{j} - \beta_{nil}^{j}}{h_i^y} - S_{nil}^{1y-} \hat{R}_{i-1}^j \frac{\beta_{nil}^{j} - \beta_{n,i-1,l}^{j}}{h_{i-1}^y} +$$

$$+ S_{nil}^{2y+} \hat{B}_i^j \frac{\beta_{n,i+1,l}^{j} - \beta_{nil}^{j}}{h_i^y} - S_{nil}^{2y-} \hat{B}_{i-1}^j \frac{\beta_{nil}^{j} - \beta_{n,i-1,l}^{j}}{h_{i-1}^y} +$$

$$+ S_{nil}^{2yd} \left(r_2\left(\beta_{nil}^{j+\frac{1}{3}} \right) \beta_{nil}^{j+\frac{1}{3}} + q_2^{j+\frac{1}{3}} \right)\Big|_{S_{nil}^{2yd}} +$$

$$+ S_{nil}^{1z+} \tilde{R}_l^j \frac{\beta_{ni,l+1}^{j} - \beta_{nil}^{j}}{h_l^z} - S_{nil}^{1z-} \tilde{R}_{l-1}^j \frac{\beta_{nil}^{j} - \beta_{ni,l-1}^{j}}{h_{l-1}^z} +$$

$$+ S_{nil}^{2z+} \tilde{B}_l^j \frac{\beta_{ni,l+1}^{j} - \beta_{nil}^{j}}{h_l^z} - S_{nil}^{2z-} \tilde{B}_{l-1}^j \frac{\beta_{nil}^{j} - \beta_{ni,l-1}^{j}}{h_{l-1}^z} +$$

$$+ S_{nil}^{2zd} \left(r_2\left(\beta_{nil}^{j+\frac{1}{3}} \right) \beta_{nil}^{j+\frac{1}{3}} + q_2^{j+\frac{1}{3}} \right)\Big|_{S_{nil}^{2zd}} \Bigg],$$

$$\begin{pmatrix} j = \overline{0, J-1}; \ n = \overline{1, N^*(m)-1}; \ i = \overline{1, I^*(m)-1}; \\ l = \overline{1, L^{**}(n,i)}, \qquad m = \overline{1, M} \end{pmatrix},$$

where $w_{nil}^{j+1} = \dfrac{\tau^{j+1}}{3V_{nil}}$.

The last relation holds for internal cells of Q whose lateral faces do not belong to its outer boundary. If any of the surfaces S_{nil}^{1x+}, $S_{nil}^{1x-}, \ldots, S_{nil}^{1z-}$ reaches the outer boundary of the domain, then the corresponding term in the heat balance equation is approximated taking into account the boundary conditions. For example, for $n = 0$, the second and fourth terms in the first square bracket in the last equality vanish (for more detail, see [11]).

The last two subproblems are approximated in a similar fashion.

The system of nonlinear algebraic equations resulting from the spatial approximation of the above-indicated three subproblems are solved consecutively in the direction x, y and z by the proposed in [2] iterative method. For this reason, the function of the temperature $\beta(E)$ in these equations is represented in the form $\beta\left(E_{nil}^j\right) = u_{nil}^j E_{nil}^j + v_{nil}^j$, where

$$u_{nil}^j = \begin{cases} 1/a_{nil}, & E_{nil}^j < a_{nil} T_1 , \\ 1/b_{nil}^1, & a_{nil} T_1 \le E_{nil}^j < d_{nil}^1 T_2 + d_{nil}^2 , \\ 1/d_{nil}^1, & E_{nil}^j \ge d_{nil}^1 T_2 + d_{nil}^2 , \end{cases}$$

$$v_{nil}^{j}=\begin{cases}0, & E_{nil}^{j}<a_{nil}T_1\,,\\ b_{nil}^{2}/b_{nil}^{1}, & a_{nil}T_1\le E_{nil}^{j}<d_{nil}^{1}T_2+d_{nil}^{2}\,,\\ -d_{nil}^{2}/d_{nil}^{1}, & E_{nil}^{j}\ge d_{nil}^{1}T_2+d_{nil}^{2}\,.\end{cases}$$

This view of the temperature function is substituted in all obtained systems of equations. Further these systems of equations are reduced to the so-called tridiagonal matrix form and are solved iteratively by applying Gaussian elimination.

Determination of the solidification front in the metal was carried out using the following algorithm. Let x_n, y_i and z_l be the coordinates of the spatial grid points. For each point $(x_n, y_i)\in S$ (where S is the projection of the phase boundary onto a plane perpendicular to the vertical axis of the mold) we find an index l_* such that one of the following conditions is satisfied:

$\left(\beta(E_{ni,l_*+1}^{j})\le T_{pl}\le\beta(E_{nil_*}^{j})\right)\cup\left(\beta(E_{nil_*}^{j})\le T_{pl}\le\beta(E_{ni,l_*+1}^{j})\right)$.

In this case we assume:

$$Z_{pl}(x_n,y_i,t^j)=\frac{(z_{l_*+1}-z_{l_*})T_{pl}+(z_{l_*}\,\beta_{ni,l_*+1}^{j}-z_{l_*+1}\,\beta_{nil_*}^{j})}{\beta_{ni,l_*+1}^{j}-\beta_{nil_*}^{j}}.$$

In the computation of the direct problem primary attention is given to the evolution of the solidification front and to how it is affected by the parameters of the problem. A special software package [12] allowed us to take a look at the dynamics of the metal crystallization process. It was developed to visualize the results of calculation of problems, in which complex dynamic processes are investigated, and allows to reflect in a video the change of an arbitrary flat scalar field over time and also distinguish arbitrary planar objects and their boundaries, which could also be moving.

IV. Solving of the Optimal Control Problem

The optimal control problem was reduced to an unconstrained optimization problem and was solved numerically with the help of gradient methods. Formulas for gradient evaluation are derived using the Fast Automatic Differentiation technique. This technique offers canonical formulas producing the exact value of the cost function gradient for a chosen discretization of the optimal control problem ([1]). It should be noted that other methods for computing the cost function gradient (for example, finite differences) were found to be hardly applicable to solving this problem.

In [2] is estimated the processor time required to compute the gradient of the objective function by means of the Fast Automatic Differentiation technique in optimal control problems for thermal processes with phase transitions. Using the example of an optimal control problem for the melting process, the assertion that the time required to find the components of the gradient of the objective function by this method does not exceed the time of calculating two values of the function is formulated and proved.

To calculate the gradient of the objective function using the Fast Automatic Differentiation technique, at first all the equations approximating the direct problem are written in a special canonical form, which is specified below.

Let us introduce the following notation. For all $i=\overline{0,I^*(m)}$, $l=\overline{0,L^*(m)}$, $m=\overline{1,M}$ let (X_m), (X_f), and (X_d) denote the $(N^*(m)+2)$-dimensional vectors:

$$(X_m)_{0il}^{j}=-\left(r_1\left(\beta_{0il}^{j}\right)\beta_{0il}^{j}+q_1^{j}\right)\Big|_{S_{0il}^{1x-}},$$

$$(X_m)_{nil}^{j}=R_{n-1}^{j}\frac{\beta_{nil}^{j}-\beta_{n-1,il}^{j}}{h_{n-1}^{x}},\quad n=\overline{1,N^*(m)},$$

$$(X_m)_{N^*(m)+1,il}^{j}=\left(r_1\left(\beta_{N^*(m)il}^{j}\right)\beta_{N^*(m)il}^{j}+q_1^{j}\right)\Big|_{S_{N^*(m)il}^{1x+}},$$

$$(X_f)_{0il}^{j}=-\left(r_2\left(\beta_{0il}^{j}\right)\beta_{0il}^{j}+q_2^{j}\right)\Big|_{S_{0il}^{2x-}},$$

$$(X_f)_{nil}^{j}=B_{n-1}^{j}\frac{\beta_{nil}^{j}-\beta_{n-1,il}^{j}}{h_{n-1}^{x}},\quad n=\overline{1,N^*(m)},$$

$$(X_f)_{N^*(m)+1,il}^{j}=\left(r_2\left(\beta_{N^*(m)il}^{j}\right)\beta_{N^*(m)il}^{j}+q_2^{j}\right)\Big|_{S_{N^*(m)il}^{2x+}},$$

$$(X_d)_{nil}^{j}=\left(r_2\left(\beta_{nil}^{j}\right)\beta_{nil}^{j}+q_2^{j}\right)\Big|_{S_{nil}^{2xd}},\quad n=\overline{0,N^*(m)+1}.$$

For all $n=\overline{0,N^*(m)}$, $l=\overline{0,L^*(m)}$, $m=\overline{1,M}$ let (Y_m), (Y_f), and (Y_d) denote the $(I^*(m)+2)$-dimensional vectors:

$$(Y_m)_{n0l}^{j}=-\left(r_1\left(\beta_{n0l}^{j}\right)\beta_{n0l}^{j}+q_1^{j}\right)\Big|_{S_{n0l}^{1y-}},$$

$$(Y_m)_{nil}^{j}=\hat{R}_{i-1}^{j}\frac{\beta_{nil}^{j}-\beta_{n,i-1,l}^{j}}{h_{i-1}^{y}},\quad i=\overline{1,I^*(m)},$$

$$(Y_m)_{n,I^*(m)+1,l}^{j}=\left(r_1\left(\beta_{nI^*(m)\,l}^{j}\right)\beta_{nI^*(m)\,l}^{j}+q_1^{j}\right)\Big|_{S_{nI^*(m)\,l}^{1y+}},$$

$$(Y_f)_{n0l}^{j}=-\left(r_2\left(\beta_{n0l}^{j}\right)\beta_{n0l}^{j}+q_2^{j}\right)\Big|_{S_{n0l}^{2y-}},$$

$$(Y_f)_{nil}^{j}=\hat{B}_{i-1}^{j}\frac{\beta_{nil}^{j}-\beta_{n,i-1,l}^{j}}{h_{i-1}^{y}},\quad i=\overline{1,I^*(m)},$$

$$(Y_f)_{n,I^*(m)+1,l}^{j}=\left(r_2\left(\beta_{nI^*(m)\,l}^{j}\right)\beta_{nI^*(m)\,l}^{j}+q_2^{j}\right)\Big|_{S_{nI^*(m)\,l}^{2y+}},$$

$$(Y_d)_{nil}^{j}=\left(r_2\left(\beta_{nil}^{j}\right)\beta_{nil}^{j}+q_2^{j}\right)\Big|_{S_{nil}^{2yd}},\quad i=\overline{0,I^*(m)+1}.$$

For all $n=\overline{0,N^*(m)}$, $i=\overline{0,I^*(m)}$, $m=\overline{1,M}$ let (Z_m), (Z_f), and (Z_d) denote the $(L^*(m)+2)$-dimensional vectors:

$$(Z_m)_{ni0}^{j}=-\left(r_1\left(\beta_{ni0}^{j}\right)\beta_{ni0}^{j}+q_1^{j}\right)\Big|_{S_{ni0}^{1z-}},$$

$$(Z_m)_{nil}^j = \tilde{R}_{l-1}^j \frac{\beta_{nil}^j - \beta_{ni,l-1}^j}{h_{l-1}^z}, \quad l = \overline{1, L^*(m)},$$

$$(Z_m)_{ni,L^*(m)+1}^j = \left(r_1\left(\beta_{niL^*(m)}^j\right)\beta_{niL^*(m)}^j + q_1^j\right)\Big|_{S_{niL^*(m)}^{1z+}},$$

$$(Z_f)_{ni0}^j = -\left(r_2\left(\beta_{ni0}^j\right)\beta_{ni0}^j + q_2^j\right)\Big|_{S_{ni0}^{2z-}},$$

$$(Z_f)_{nil}^j = \tilde{B}_{l-1}^j \frac{\beta_{nil}^j - \beta_{ni,l-1}^j}{h_{l-1}^z}, \quad l = \overline{1, L^*(m)},$$

$$(Z_f)_{ni,L^*(m)+1}^j = \left(r_2\left(\beta_{niL^*(m)}^j\right)\beta_{niL^*(m)}^j + q_2^j\right)\Big|_{S_{niL^*(m)}^{2z+}},$$

$$(Z_d)_{nil}^j = \left(r_2\left(\beta_{nil}^j\right)\beta_{nil}^j + q_2^j\right)\Big|_{S_{nil}^{2zd}}, \quad l = \overline{0, L^*(m)+1}.$$

In these and subsequent formulas, the subscripts m and f denote the metal and the mold, respectively. The index d says that the right-hand side of the corresponding equality is calculated at the center of an additional surface for cells of complex geometry.

With the notation introduced, the approximations of the above three subproblems can be written for all $j = \overline{0, J-1}$ as follows:

x-direction:

$$E_{nil}^{j+1/3} = E_{nil}^j + w_{nil}^{j+1}\left[S_{nil}^{1x+}\cdot(X_m)_{n+1,il}^{j+1/3} - S_{nil}^{1x-}\cdot(X_m)_{nil}^{j+1/3} + \right.$$
$$\left. + S_{nil}^{2x+}\cdot(X_f)_{n+1,il}^{j+1/3} - S_{nil}^{2x-}\cdot(X_f)_{nil}^{j+1/3} + S_{nil}^{2xd}\cdot(X_d)_{nil}^{j+1/3}\right] +$$
$$+ w_{nil}^{j+1}\left[S_{nil}^{1y+}\cdot(Y_m)_{n,i+1,l}^j - S_{nil}^{1y-}\cdot(Y_m)_{nil}^j + S_{nil}^{2y+}\cdot(Y_f)_{n,i+1,l}^j\right] +$$
$$+ w_{nil}^{j+1}\left[- S_{nil}^{2y-}\cdot(Y_f)_{nil}^j + S_{nil}^{2yd}\cdot(Y_d)_{nil}^j\right] +$$
$$+ w_{nil}^{j+1}\left[S_{nil}^{1z+}\cdot(Z_m)_{ni,l+1}^j - S_{nil}^{1z-}\cdot(Z_m)_{nil}^j + S_{nil}^{2z+}\cdot(Z_f)_{ni,l+1}^j\right]$$
$$+ w_{nil}^{j+1}\left[- S_{nil}^{2z-}\cdot(Z_f)_{nil}^j + S_{nil}^{2zd}\cdot(Z_d)_{nil}^j\right],$$
$$n = \overline{0, N^*(m)}, \quad i = \overline{0, I^*(m)}, \quad l = \overline{0, L^*(m)}, \quad m = \overline{1, M};$$

y-direction:

$$E_{nil}^{j+2/3} = E_{nil}^{j+1/3} + w_{nil}^{j+1}\left[S_{nil}^{1y+}\cdot(Y_m)_{n,i+1,l}^{j+2/3} - S_{nil}^{1y-}\cdot(Y_m)_{nil}^{j+2/3} + \right.$$
$$\left. + S_{nil}^{2y+}\cdot(Y_f)_{n,i+1,l}^{j+2/3} - S_{nil}^{2y-}\cdot(Y_f)_{nil}^{j+2/3} + S_{nil}^{2yd}\cdot(Y_d)_{nil}^{j+2/3}\right] +$$
$$+ w_{nil}^{j+1}\left[S_{nil}^{1x+}\cdot(X_m)_{n+1,il}^{j+1/3} - S_{nil}^{1x-}\cdot(X_m)_{nil}^{j+1/3} + S_{nil}^{2x+}\cdot(X_f)_{n+1,il}^{j+1/3}\right] +$$
$$+ w_{nil}^{j+1}\left[- S_{nil}^{2x-}\cdot(X_f)_{nil}^{j+1/3} + S_{nil}^{2xd}\cdot(X_d)_{nil}^{j+1/3}\right] +$$
$$+ w_{nil}^{j+1}\left[S_{nil}^{1z+}\cdot(Z_m)_{ni,l+1}^{j+1/3} - S_{nil}^{1z-}\cdot(Z_m)_{nil}^{j+1/3} + S_{nil}^{2z+}\cdot(Z_f)_{ni,l+1}^{j+1/3}\right]$$
$$+ w_{nil}^{j+1}\left[- S_{nil}^{2z-}\cdot(Z_f)_{nil}^{j+1/3} + S_{nil}^{2zd}\cdot(Z_d)_{nil}^{j+1/3}\right],$$
$$n = \overline{0, N^*(m)}, \quad i = \overline{0, I^*(m)}, \quad l = \overline{0, L^*(m)}, \quad m = \overline{1, M};$$

z-direction:

$$E_{nil}^{j+1} = E_{nil}^{j+2/3} + w_{nil}^{j+1}\left[S_{nil}^{1z+}\cdot(Z_m)_{ni,l+1}^{j+1} - S_{nil}^{1z-}\cdot(Z_m)_{nil}^{j+1} + \right.$$
$$\left. + S_{nil}^{2z+}\cdot(Z_f)_{ni,l+1}^{j+1} - S_{nil}^{2z-}\cdot(Z_f)_{nil}^{j+1} + S_{nil}^{2zd}\cdot(Z_d)_{nil}^{j+1}\right] +$$
$$+ w_{nil}^{j+1}\left[S_{nil}^{1x+}\cdot(X_m)_{n+1,il}^{j+2/3} - S_{nil}^{1x-}\cdot(X_m)_{nil}^{j+2/3} + S_{nil}^{2x+}\cdot(X_f)_{n+1,il}^{j+2/3}\right] +$$
$$+ w_{nil}^{j+1}\left[- S_{nil}^{2x-}\cdot(X_f)_{nil}^{j+2/3} + S_{nil}^{2xd}\cdot(X_d)_{nil}^{j+2/3}\right] +$$
$$+ w_{nil}^{j+1}\left[S_{nil}^{1y+}\cdot(Y_m)_{n,i+1,l}^{j+2/3} - S_{nil}^{1y-}\cdot(Y_m)_{nil}^{j+2/3} + S_{nil}^{2y+}\cdot(Y_f)_{n,i+1,l}^{j+2/3}\right]$$
$$+ w_{nil}^{j+1}\left[- S_{nil}^{2y-}\cdot(Y_f)_{nil}^{j+2/3} + S_{nil}^{2yd}\cdot(Y_d)_{nil}^{j+2/3}\right],$$
$$n = \overline{0, N^*(m)}, \quad i = \overline{0, I^*(m)}, \quad l = \overline{0, L^*(m)}, \quad m = \overline{1, M}.$$

Define the two-dimensional vectors

$$S_{nil}^{x+} = \begin{bmatrix} S_{nil}^{1x+} \\ S_{nil}^{2x+} \end{bmatrix}, \quad S_{nil}^{x-} = \begin{bmatrix} S_{nil}^{1x-} \\ S_{nil}^{2x-} \end{bmatrix}, \quad S_{nil}^{y+} = \begin{bmatrix} S_{nil}^{1y+} \\ S_{nil}^{2y+} \end{bmatrix},$$

$$S_{nil}^{y-} = \begin{bmatrix} S_{nil}^{1y-} \\ S_{nil}^{2y-} \end{bmatrix}, \quad S_{nil}^{z+} = \begin{bmatrix} S_{nil}^{1z+} \\ S_{nil}^{2z+} \end{bmatrix}, \quad S_{nil}^{z-} = \begin{bmatrix} S_{nil}^{1z-} \\ S_{nil}^{2z-} \end{bmatrix},$$

$$(X_{mf})_{nil}^j = \begin{bmatrix} (X_m)_{nil}^j \\ (X_f)_{nil}^j \end{bmatrix}, \ (Y_{mf})_{nil}^j = \begin{bmatrix} (Y_m)_{nil}^j \\ (Y_f)_{nil}^j \end{bmatrix}, \ (Z_{mf})_{nil}^j = \begin{bmatrix} (Z_m)_{nil}^j \\ (Z_f)_{nil}^j \end{bmatrix},$$

where $n = \overline{0, N^*(m)}, \quad i = \overline{0, I^*(m)}, \quad l = \overline{0, L^*(m)}, \quad m = \overline{1, M}$.

Note that $S_{nil}^{x+} = S_{n+1,il}^{x-}$, ($n = \overline{0, N^*(m)-1}$); $S_{nil}^{y+} = S_{n,i+1,l}^{y-}$, ($i = \overline{0, I^*(m)-1}$); and $S_{nil}^{z+} = S_{ni,l+1}^{z-}$, ($l = \overline{0, L^*(m)-1}$), where $m = \overline{1, M}$.

We also introduce notation for the following scalar products (for all $m = \overline{1, M}$):

$$\tilde{X}_{nil}^j = \left(S_{nil}^{x-}, (X_{mf})_{nil}^j\right), \qquad n = \overline{0, N^*(m)},$$
$$\tilde{X}_{N^*(m)+1,il}^j = \left(S_{N^*(m)il}^{x+}, (X_{mf})_{N^*(m)+1,il}^j\right),$$
$$i = \overline{0, I^*(m)}, \quad l = \overline{0, L^*(m)};$$
$$\tilde{Y}_{nil}^j = \left(S_{nil}^{y-}, (Y_{mf})_{nil}^j\right), \qquad i = \overline{0, I^*(m)},$$
$$\tilde{Y}_{n,I^*(m)+1,l}^j = \left(S_{nI^*(m)l}^{y+}, (Y_{mf})_{n,I^*(m)+1,l}^j\right),$$
$$n = \overline{0, N^*(m)}, \quad l = \overline{0, L^*(m)};$$
$$\tilde{Z}_{nil}^j = \left(S_{nil}^{z-}, (Z_{mf})_{nil}^j\right), \qquad l = \overline{0, L^*(m)},$$
$$\tilde{Z}_{ni,L^*(m)+1}^j = \left(S_{niL^*(m)}^{z+}, (Z_{mf})_{ni,L^*(m)+1}^j\right),$$
$$n = \overline{0, N^*(m)}, \quad i = \overline{0, I^*(m)}.$$

With the notation introduced, the last three subproblems can be written in the following compact form:

x-direction:

$$E_{nil}^{j+1/3} = E_{nil}^j + w_{nil}^{j+1}\left(\tilde{X}_{n+1,il}^{j+1/3} - \tilde{X}_{nil}^{j+1/3} + S_{nil}^{2xd}\cdot(X_d)_{nil}^{j+1/3}\right) +$$
$$+ w_{nil}^{j+1}\left(\tilde{Y}_{n,i+1,l}^j - \tilde{Y}_{nil}^j + S_{nil}^{2yd}\cdot(Y_d)_{nil}^j\right) +$$
$$+ w_{nil}^{j+1}\left(\tilde{Z}_{ni,l+1}^j - \tilde{Z}_{nil}^j + S_{nil}^{2zd}\cdot(Z_d)_{nil}^j\right), \tag{4}$$

y-direction:

$$E_{nil}^{j+2/3} = E_{nil}^{j+1/3} + w_{nil}^{j+1}\left(\tilde{Y}_{n,i+1,l}^{j+2/3} - \tilde{Y}_{nil}^{j+2/3} + S_{nil}^{2yd}\cdot\left(Y_d\right)_{nil}^{j+2/3}\right) + \\ + w_{nil}^{j+1}\left(\tilde{X}_{n+1,il}^{j+1/3} - \tilde{X}_{nil}^{j+1/3} + S_{nil}^{2xd}\cdot\left(X_d\right)_{nil}^{j+1/3}\right) + \\ + w_{nil}^{j+1}\left(\tilde{Z}_{ni,l+1}^{j+1/3} - \tilde{Z}_{nil}^{j+1/3} + S_{nil}^{2zd}\cdot\left(Z_d\right)_{nil}^{j+1/3}\right), \quad (5)$$

z-direction:

$$E_{nil}^{j+1} = E_{nil}^{j+2/3} + w_{nil}^{j+1}\left(\tilde{Z}_{ni,l+1}^{j+1} - \tilde{Z}_{nil}^{j+1} + S_{nil}^{2zd}\cdot\left(Z_d\right)_{nil}^{j+1}\right) + \\ + w_{nil}^{j+1}\left(\tilde{X}_{n+1,il}^{j+2/3} - \tilde{X}_{nil}^{j+2/3} + S_{nil}^{2xd}\cdot\left(X_d\right)_{nil}^{j+2/3}\right) + \\ + w_{nil}^{j+1}\left(\tilde{Y}_{n,i+1,l}^{j+2/3} - \tilde{Y}_{nil}^{j+2/3} + S_{nil}^{2yd}\cdot\left(Y_d\right)_{nil}^{j+2/3}\right), \quad (6)$$

$$n = \overline{0, N^*(m)}, \quad i = \overline{0, I^*(m)}, \quad l = \overline{0, L^*(m)}, \quad m = \overline{1, M};$$
$$j = \overline{0, J-1}.$$

Equations (4)-(6) are the canonical form of the chosen discrete version of the direct problem.

The cost functional $I(u)$ is approximated by a function $F(u)$ with the help of the trapezoidal formula:

$$I(u) \cong F(u) = \frac{1}{2(t_2 - t_1)}\left(\tau^{j_1+1} f^{j_1} + \sum_{j=j_1+1}^{j_2-1}\left(\tau^j + \tau^{j+1}\right) f^j + \tau^{j_2} f^{j_2}\right).$$

Here, j_1 is the index of the time grid point corresponding to the time t_1; j_2 is the index of the time grid point corresponding to the time t_2;

$$f^j = \sum_{n=n_1}^{n_2}\sum_{i=i_1}^{i_2}\left(Z_{ni}^j - z_*^j\right)^2 h_n^x h_i^y;$$

$Z_{ni}^j = Z_{pl}(x_n, y_i, t^j)$, $z_*^j = z_*(t^j)$; n_1, n_2, i_1, and i_2 are the indices of the spatial grid points along the OX and OY axes, respectively, that define the boundaries of the cross section (the largest cross section of the metal filled part of the object); i.e., $mes\hat{S} = (x_{n_2} - x_{n_1}) \times (y_{i_2} - y_{i_1})$. The value $Z_{pl}(x_n, y_i, t^j)$ is defined at the end of the third section.

According to the Fast Automatic Differentiation technique, each equation of the chosen discrete version of the direct problem (4)–(6) is written as

$$E_{nil}^j = \Psi\left((n,i,l,j), \Lambda_{(n,i,l,j)}, U_{(n,i,l,j)}\right). \quad (7)$$

Here, $\Lambda_{(n,i,l,j)}$ denotes the set of all $E_{\alpha\beta\gamma}^{\nu}$ (with all indices α, β, γ, and ν,) that enter into the right-hand side of (7), and $U_{(n,i,l,j)}$ is the set of all components of u^{ν} $\left(u^{\nu} = u(t^{\nu})\right)$ that enter into the right-hand side of (7). Although the control u^j depends only on the time index j, the set $U_{(n,i,l,j)}$ is equipped with the spatial indices n, i, and l to stress that the effect of this control is different at different spatial points.

The components of the gradient of $F(u)$ are computed from the components of the vector $\{u^j\}$ by using the following relation, which is a generalization of that used in [1]:

$$\frac{dF}{du^j} = \frac{\partial F}{\partial u^j} + \\ + \sum_{(\alpha,\beta,\gamma,\nu)\in\bar{K}_{(n,i,l,j)}} \Psi_{u^j}^T\left((\alpha,\beta,\gamma,\nu), \Lambda_{(\alpha,\beta,\gamma,\nu)}, U_{(\alpha,\beta,\gamma,\nu)}\right) p_{\alpha\beta\gamma}^{\nu}, \quad (8)$$

where $p_{\alpha\beta\gamma}^{\nu}$ are the conjugate variables determined by solving the system of linear algebraic equations

$$p_{nil}^j = \frac{\partial F}{\partial E_{nil}^j} + \\ + \sum_{(\alpha,\beta,\gamma,\nu)\in\bar{Q}_{(n,i,l,j)}} \Psi_{E_{nil}^j}^T\left((\alpha,\beta,\gamma,\nu), \Lambda_{(\alpha,\beta,\gamma,\nu)}, U_{(\alpha,\beta,\gamma,\nu)}\right) p_{\alpha\beta\gamma}^{\nu}, \quad (9)$$

$$j = \overline{1, J},\ n = \overline{0, N^*(m)},\ i = \overline{0, I^*(m)},\ l = \overline{0, L^*(m)},\ m = \overline{1, M}.$$

The index sets $\bar{Q}_{(n,i,l,j)}$ and $\bar{K}_{(n,i,l,j)}$ are given by

$$\bar{Q}_{(n,i,l,j)} = \left\{(\alpha,\beta,\gamma,\nu) : E_{nil}^j \in \Lambda_{(\alpha,\beta,\gamma,\nu)}\right\},$$
$$\bar{K}_{(n,i,l,j)} = \left\{(\alpha,\beta,\gamma,\nu) : u^j \in U_{(\alpha,\beta,\gamma,\nu)}\right\}.$$

System (9) for computing the conjugate variables p_{nil}^j is usually called the adjoint problem.

We introduce the following notation for some derivatives, which is used to represent the adjoint problem in a compact form:

$$\left(D_{x+}\right)_{nil}^j = \frac{\partial \tilde{X}_{nil}^j}{\partial E_{nil}^j}, \quad \left(D_{x-}\right)_{nil}^j = \frac{\partial \tilde{X}_{nil}^j}{\partial E_{n-1,il}^j}, \quad n = \overline{1, N^*(m)},$$

$$\left(D_{x+}\right)_{0il}^j = \frac{\partial \tilde{X}_{0il}^j}{\partial E_{0il}^j}, \qquad \left(D_{x-}\right)_{0il} = 0,$$

$$\left(D_{x+}\right)_{N^*(m)+1,il}^j = 0, \qquad \left(D_{x-}\right)_{N^*(m)+1,il}^j = \frac{\partial \tilde{X}_{N^*(m)+1,il}^j}{\partial E_{N^*(m)il}^j},$$

$$\forall\ i = \overline{0, I^*(m)} \text{ and } \forall\ l = \overline{0, L^*(m)} \qquad (m = \overline{1, M});$$

$$\left(D_{y+}\right)_{nil}^j = \frac{\partial \tilde{Y}_{nil}^j}{\partial E_{nil}^j}, \quad \left(D_{y-}\right)_{nil}^j = \frac{\partial \tilde{Y}_{nil}^j}{\partial E_{n,i-1,l}^j}, \quad i = \overline{1, I^*(m)},$$

$$\left(D_{y+}\right)_{n0l}^j = \frac{\partial \tilde{Y}_{n0l}^j}{\partial E_{n0l}^j}, \qquad \left(D_{y-}\right)_{n0l}^j = 0,$$

$$\left(D_{y+}\right)_{n,I^*(m)+1,l}^j = 0, \qquad \left(D_{y-}\right)_{n,I^*(m)+1,l}^j = \frac{\partial \tilde{Y}_{n,I^*(m)+1,l}^j}{\partial E_{nI^*(m)l}^j};$$

$\forall\ n=\overline{0,N^*(m)}$ and $\forall\ l=\overline{0,L^*(m)}$ $\quad (m=\overline{1,M})$;

$$(D_{z+})^j_{nil}=\frac{\partial \tilde{Z}^j_{nil}}{\partial E^j_{nil}},\quad (D_{z-})^j_{nil}=\frac{\partial \tilde{Z}^j_{nil}}{\partial E^j_{ni,l-1}},\qquad l=\overline{1,L^*(m)},$$

$$(D_{z+})^j_{ni0}=\frac{\partial \tilde{Z}^j_{ni0}}{\partial E^j_{ni0}},\qquad (D_{z-})^j_{ni0}=0,$$

$$(D_{z+})^j_{ni,L^*(m)+1}=0,\qquad (D_{z-})^j_{ni,L^*(m)+1}=\frac{\partial \tilde{Z}^j_{ni,L^*(m)+1}}{\partial E^j_{niL^*(m)}};$$

$\forall\ n=\overline{0,N^*(m)}$ and $\forall\ i=\overline{0,I^*(m)}$ $\quad (m=\overline{1,M})$;

$$(D_{xd})^j_{nil}=\frac{\partial (X_d)^j_{nil}}{\partial E^j_{nil}},\qquad (D_{yd})^j_{nil}=\frac{\partial (Y_d)^j_{nil}}{\partial E^j_{nil}},$$

$$(D_{zd})^j_{nil}=\frac{\partial (Z_d)^j_{nil}}{\partial E^j_{nil}}.$$

$\forall n=\overline{0,N^*(m)},\ \forall i=\overline{0,I^*(m)},\ \forall l=\overline{0,L^*(m)},\ m=\overline{1,M}$.

In [11] a detailed description of the conjugate equations is given, which are obtained in the case of studying the object of the simplest form - a parallelepiped. Here we give a compact form of the adjoint problem for calculating the quantities p^j_{nil} in the case of the object of complex geometric form, which is represented in Fig. 1. The compact form of these equations is possible, if we formally assume:

$$p^j_{-1,il}=p^j_{N^*(m)+1,il}=p^j_{n,-1,l}=p^j_{n,I^*(m)+1,l}=$$
$$=p^j_{ni,-1}=p^j_{ni,L^*(m)+1}=0,$$
$$p^{j+1/3}_{-1,il}=p^{j+1/3}_{N^*(m)+1,il}=p^{j+1/3}_{n,-1,l}=p^{j+1/3}_{n,I^*(m)+1,l}=$$
$$=p^{j+1/3}_{ni,-1}=p^{j+1/3}_{ni,L^*(m)+1}=0,$$
$$p^{j+2/3}_{-1,il}=p^{j+2/3}_{N^*(m)+1,il}=p^{j+2/3}_{n,-1,l}=p^{j+2/3}_{n,I^*(m)+1,l}=$$
$$=p^{j+2/3}_{ni,-1}=p^{j+2/3}_{ni,L^*(m)+1}=0,$$

$$(n=\overline{0,N^*(m)},\quad i=\overline{0,I^*(m)},\quad l=\overline{0,L^*(m)},\quad j=\overline{1,J},\quad m=\overline{1,M}).$$

Initial Conditions for the Conjugate Variables

To obtain the conjugate variables at the last time level $j=J$, the following system of linear algebraic equations is solved for p^J_{nil} with all $\forall n=\overline{0,N^*(m)}$ and all $\forall i=\overline{0,I^*(m)}$, $(m=\overline{1,M})$:

$$\begin{aligned}p^J_{nil}&=w^J_{ni,l-1}(D_{z+})^J_{nil}\,p^J_{ni,l-1}+w^J_{nil}(D_{z-})^J_{ni,l+1}\,p^J_{nil}-\\&-w^J_{nil}(D_{z+})^J_{nil}\,p^J_{nil}-w^J_{ni,l+1}(D_{z-})^J_{ni,l+1}\,p^J_{ni,l+1}+\\&+w^J_{nil}S^{2zd}_{nil}(D_{zd})^J_{nil}\,p^J_{nil}+\partial F/\partial E^J_{nil},\\&l=\overline{0,L^{**}(n,i)}.\end{aligned}\tag{10}$$

First Subproblem for the Conjugate Variables

The conjugate variables $p^{j+2/3}_{nil}$ at the time sublevel $(j+2/3)$, $j=\overline{J-1,0}$, are computed by solving the following linear algebraic system of equations for all $n=\overline{0,N^*(m)}$ and all $l=\overline{0,L^*(m)}$, $(m=\overline{1,M})$:

$$\begin{aligned}p^{j+2/3}_{nil}&=w^{j+1}_{n,i-1,l}(D_{y+})^{j+2/3}_{nil}\,p^{j+2/3}_{n,i-1,l}+\\&+w^{j+1}_{nil}\left((D_{y-})^{j+2/3}_{n,i+1,l}-(D_{y+})^{j+2/3}_{nil}\right)p^{j+2/3}_{nil}-\\&-w^{j+1}_{n,i+1,l}(D_{y-})^{j+2/3}_{n,i+1,l}\,p^{j+2/3}_{n,i+1,l}+\\&+w^{j+1}_{nil}S^{2yd}_{nil}(D_{yd})^{j+2/3}_{nil}\,p^{j+2/3}_{nil}+\xi^{j+2/3}_{nil},\end{aligned}\tag{11}$$

where

$$\begin{aligned}\xi^{j+2/3}_{nil}&=p^{j+1}_{nil}+w^{j+1}_{n-1,il}(D_{x+})^{j+2/3}_{nil}\,p^{j+1}_{n-1,il}+\\&+w^{j+1}_{nil}\left((D_{x-})^{j+2/3}_{n+1,il}-(D_{x+})^{j+2/3}_{nil}\right)p^{j+1}_{nil}-\\&-w^{j+1}_{n+1,il}(D_{x-})^{j+2/3}_{n+1,il}\,p^{j+1}_{n+1,il}+\\&+w^{j+1}_{n,i-1,l}(D_{y+})^{j+2/3}_{nil}\,p^{j+1}_{n,i-1,l}+\\&+w^{j+1}_{nil}\left((D_{y-})^{j+2/3}_{n,i+1,l}-(D_{y+})^{j+2/3}_{nil}\right)p^{j+1}_{nil}-\\&-w^{j+1}_{n,i+1,l}(D_{y-})^{j+2/3}_{n,i+1,l}\,p^{j+1}_{n,i+1,l}+\\&+w^{j+1}_{nil}S^{2xd}_{nil}(D_{xd})^{j+2/3}_{nil}\,p^{j+1}_{nil}+\\&+w^{j+1}_{nil}S^{2yd}_{nil}(D_{yd})^{j+2/3}_{nil}\,p^{j+1}_{nil}+\frac{\partial F}{\partial E^{j+2/3}_{nil}},\\&i=\overline{0,I^*(m)}.\end{aligned}$$

Second Subproblem for the Conjugate Variables

The conjugate variables $p^{j+1/3}_{nil}$ at the time sublevel $(j+1/3)$, $j=\overline{J-1,0}$, are computed by solving the following linear algebraic system of equations for all $i=\overline{0,I^*(m)}$ and all $l=\overline{0,L^*(m)}$, $(m=\overline{1,M})$:

$$\begin{aligned}p^{j+1/3}_{nil}&=w^{j+1}_{n-1,il}(D_{x+})^{j+1/3}_{nil}\,p^{j+1/3}_{n-1,il}+\\&+w^{j+1}_{nil}\left((D_{x-})^{j+1/3}_{n+1,il}-(D_{x+})^{j+1/3}_{nil}\right)p^{j+1/3}_{nil}-\\&-w^{j+1}_{n+1,il}(D_{x-})^{j+1/3}_{n+1,il}\,p^{j+1/3}_{n+1,il}+\\&+w^{j+1}_{nil}S^{2xd}_{nil}(D_{xd})^{j+1/3}_{nil}\,p^{j+1/3}_{nil}+\xi^{j+1/3}_{nil},\end{aligned}\tag{12}$$

$$\begin{aligned}\xi_{nil}^{j+1/3} = p_{nil}^{j+2/3} &+ w_{n-1,il}^{j+1}(D_{x+})_{nil}^{j+1/3} p_{n-1,il}^{j+2/3} + \\ &+ w_{nil}^{j+1}\left((D_{x-})_{n+1,il}^{j+1/3} - (D_{x+})_{nil}^{j+1/3}\right)p_{nil}^{j+2/3} - \\ &- w_{n+1,il}^{j+1}(D_{x-})_{n+1,il}^{j+1/3} p_{n+1,il}^{j+2/3} + \\ &+ w_{nil}^{j+1} S_{nil}^{2xd}(D_{xd})_{nil}^{j+1/3} p_{nil}^{j+2/3} + \\ &+ w_{ni,l-1}^{j+1}(D_{z+})_{nil}^{j+1/3} p_{ni,l-1}^{j+2/3} + \\ &+ w_{nil}^{j+1}\left((D_{z-})_{ni,l+1}^{j+1/3} - (D_{z+})_{nil}^{j+1/3}\right)p_{nil}^{j+2/3} - \\ &- w_{ni,l+1}^{j+1}(D_{z-})_{ni,l+1}^{j+1/3} p_{ni,l+1}^{j+2/3} + \\ &+ w_{nil}^{j+1} S_{nil}^{2zd}(D_{zd})_{nil}^{j+1/3} p_{nil}^{j+2/3} + \partial F / \partial E_{nil}^{j+1/3}, \\ &n = \overline{0, N^*(m)}.\end{aligned}$$

Third Subproblem for the Conjugate Variables

The conjugate variables p_{nil}^{j} at the jth time level, $(j = \overline{J-1,0})$, are computed by solving the following linear algebraic system of equations for all $i = \overline{0, I^*(m)}$ and all $l = \overline{0, L^*(m)}$, $(m = \overline{1,M})$:

$$\begin{aligned}p_{nil}^{j} = w_{ni,l-1}^{j}(D_{z+})_{nil}^{j} p_{ni,l-1}^{j} &+ \\ + w_{nil}^{j}\left((D_{z-})_{ni,l+1}^{j} - (D_{z+})_{nil}^{j}\right)p_{nil}^{j} &- \\ - w_{ni,l+1}^{j}(D_{z-})_{ni,l+1}^{j} p_{ni,l+1}^{j} &+ \\ + w_{nil}^{j} S_{nil}^{2zd}(D_{zd})_{nil}^{j} p_{nil}^{j} &+ \xi_{nil}^{j},\end{aligned} \tag{13}$$

$$\begin{aligned}\xi_{nil}^{j} = p_{nil}^{j+1/3} &+ w_{n,i-1,l}^{j+1}(D_{y+})_{nil}^{j} p_{n,i-1,l}^{j+1/3} + \\ &+ w_{nil}^{j+1}\left((D_{y-})_{n,i+1,l}^{j} - (D_{y+})_{nil}^{j}\right)p_{nil}^{j+1/3} - \\ &- w_{n,i+1,l}^{j+1}(D_{y-})_{n,i+1,l}^{j} p_{n,i+1,l}^{j+1/3} + \\ &+ w_{nil}^{j+1} S_{nil}^{2yd}(D_{yd})_{nil}^{j} p_{nil}^{j+1/3} + \\ &+ w_{ni,l-1}^{j+1}(D_{z+})_{nil}^{j} p_{ni,l-1}^{j+1/3} + \\ &+ w_{nil}^{j+1}\left((D_{z-})_{ni,l+1}^{j} - (D_{z+})_{nil}^{j}\right)p_{nil}^{j+1/3} - \\ &- w_{ni,l+1}^{j+1}(D_{z-})_{ni,l+1}^{j} p_{ni,l+1}^{j+1/3} + \\ &+ w_{nil}^{j+1} S_{nil}^{2zd}(D_{zd})_{nil}^{j} p_{nil}^{j+1/3} + \frac{\partial F}{\partial E_{nil}^{j}}, \\ &l = \overline{0, L^{**}(n,i)}.\end{aligned}$$

The obtained systems of linear equations for the conjugate variables are the discrete version of the continuous adjoint problem, which is consistent with the approximations of the direct problem and of the cost functional. These systems of linear algebraic equations were solved using tridiagonal Gaussian elimination (see [9]). The sequential solution to these three subproblems at $j = \overline{J,0}$ produces conjugate variables in the following order: p_{nil}^{J}, $p_{nil}^{(J-1)+2/3}$, $p_{nil}^{(J-1)+1/3}$, p_{nil}^{J-1},…, $p_{nil}^{1+1/3}$, p_{nil}^{1}, $p_{nil}^{0+2/3}$, $p_{nil}^{0+1/3}$, $n = \overline{0, N^*(m)}$, $i = \overline{0, I^*(m)}$, $l = \overline{0, L^*(m)}$, $m = \overline{1,M}$.

The derivatives $(D_{x+})_{nil}^{j}$, $(D_{x-})_{nil}^{j}$,…, and the derivatives of the cost function $\partial F / \partial E_{nil}^{j}$ with respect to the state variables are computed in a similar manner, as was shown in [11].

The Gradient of the Cost Function of the Discrete Optimal Control Problem

The control function $u(t)$ in the optimal control problem is defined as the time dependent displacement of the mold in the furnace, namely, the z coordinate $Z_{Sou}(t)$ of the furnace's lower wall. This parameter is involved in the expressions for $q_1(t)$ and $q_2(t)$ for cells that are outside the liquid aluminum. The control function $u(t)$ is approximated by a piecewise linear function. More specifically, the control function on the time interval $\left[t^{j}, t^{j+1}\right]$ has the form $u(t) = Z_{Sou}(t^{j+1}) = Z_{Sou}^{j+1}$. Therefore, $q_1^{j+1/3} = q_1^{j+2/3} = q_1^{j+1}$ and $q_2^{j+1/3} = q_2^{j+2/3} = q_2^{j+1}$.

According to the Fast Automatic Differentiation technique (8), the components of the function gradient are calculated by the formula

$$\begin{aligned}\frac{dF}{du^{j}} = \frac{\partial F}{\partial u^{j}} &+ \\ + \sum_{m=1}^{M}\sum_{n=0}^{N^*(m)}\sum_{i=0}^{I^*(m)}&\left(w_{niL^*(m)}^{j}\frac{\partial \tilde{Z}_{ni,L^*(m)+1}^{j}}{\partial u^{j}}p_{niL^*(m)}^{j}\right) + \\ + \sum_{m=1}^{M}\sum_{n=0}^{N^*(m)}\sum_{i=0}^{I^*(m)}&\left(-w_{ni0}^{j}\frac{\partial \tilde{Z}_{ni0}^{j}}{\partial u^{j}}p_{ni0}^{j}\right) + \\ + \sum_{m=1}^{M}\sum_{n=0}^{N^*(m)}\sum_{l=0}^{L^*(m)}&\left(w_{nI^*(m)l}^{j}\frac{\partial \tilde{Y}_{n,I^*(m)+1,l}^{(j-1)+2/3}}{\partial u^{j}}p_{nI^*(m)l}^{j}\right) + \\ + \sum_{m=1}^{M}\sum_{n=0}^{N^*(m)}\sum_{l=0}^{L^*(m)}&\left(-w_{n0l}^{j}\frac{\partial \tilde{Y}_{n0l}^{(j-1)+2/3}}{\partial u^{j}}p_{n0l}^{j}\right) +\end{aligned}$$

$$+\sum_{m=1}^{M}\sum_{i=0}^{I^*(m)}\sum_{l=0}^{L^*(m)}\left(w_{N^*(m)il}^{j} \frac{\partial \tilde{X}_{N^*(m)+1,il}^{(j-1)+2/3}}{\partial u^j} p_{N^*(m)il}^{j} \right)+$$

$$+\sum_{m=1}^{M}\sum_{i=0}^{I^*(m)}\sum_{l=0}^{L^*(m)}\left(-w_{0il}^{j} \frac{\partial \tilde{X}_{0il}^{(j-1)+2/3}}{\partial u^j} p_{0il}^{j} \right)+$$

$$+\sum_{m=1}^{M}\sum_{n=0}^{N^*(m)}\sum_{i=0}^{I^*(m)}\sum_{l=0}^{L^*(m)} w_{nil}^{j}\left(S_{nil}^{2zd} \frac{\partial (Z_d)_{nil}^{j}}{\partial u^j} \right) p_{nil}^{j} +$$

$$+\sum_{m=1}^{M}\sum_{n=0}^{N^*(m)}\sum_{i=0}^{I^*(m)}\sum_{l=0}^{L^*(m)} w_{nil}^{j}\left(S_{nil}^{2xd} \frac{\partial (X_d)_{nil}^{(j-1)+\frac{2}{3}}}{\partial u^j} \right) p_{nil}^{j} +$$

$$+\sum_{m=1}^{M}\sum_{n=0}^{N^*(m)}\sum_{i=0}^{I^*(m)}\sum_{l=0}^{L^*(m)} w_{nil}^{j}\left(S_{nil}^{2yd} \frac{\partial (Y_d)_{nil}^{(j-1)+\frac{2}{3}}}{\partial u^j} \right) p_{nil}^{j} +$$

$$+\sum_{m=1}^{M}\sum_{n=0}^{N^*(m)}\sum_{l=0}^{L^*(m)}\left(w_{nI^*(m)l}^{j} \frac{\partial \tilde{Y}_{n,I^*(m)+1,l}^{(j-1)+\frac{2}{3}}}{\partial u^j} p_{nI^*(m)l}^{(j-1)+\frac{2}{3}} \right)+$$

$$+\sum_{m=1}^{M}\sum_{n=0}^{N^*(m)}\sum_{l=0}^{L^*(m)}\left(-w_{n0l}^{j} \frac{\partial \tilde{Y}_{n0l}^{(j-1)+\frac{2}{3}}}{\partial u^j} p_{n0l}^{(j-1)+\frac{2}{3}} \right)+$$

$$+\sum_{m=1}^{M}\sum_{i=0}^{I^*(m)}\sum_{l=0}^{L^*(m)}\left(w_{N^*(m)il}^{j} \frac{\partial \tilde{X}_{N^*(m)+1,il}^{(j-1)+\frac{1}{3}}}{\partial u^j} p_{N^*(m)il}^{(j-1)+\frac{2}{3}} \right)+$$

$$+\sum_{m=1}^{M}\sum_{i=0}^{I^*(m)}\sum_{l=0}^{L^*(m)}\left(-w_{0il}^{j} \frac{\partial \tilde{X}_{0il}^{(j-1)+\frac{1}{3}}}{\partial u^j} p_{0il}^{(j-1)+\frac{2}{3}} \right)+$$

$$+\sum_{m=1}^{M}\sum_{n=0}^{N^*(m)}\sum_{i=0}^{I^*(m)}\left(w_{niL^*(m)}^{j} \frac{\partial \tilde{Z}_{ni,L^*(m)+1}^{(j-1)+\frac{1}{3}}}{\partial u^j} p_{niL^*(m)}^{(j-1)+\frac{2}{3}} \right)+$$

$$+\sum_{m=1}^{M}\sum_{n=0}^{N^*(m)}\sum_{i=0}^{I^*(m)}\left(-w_{ni0}^{j} \frac{\partial \tilde{Z}_{ni0}^{(j-1)+\frac{1}{3}}}{\partial u^j} p_{ni0}^{(j-1)+\frac{2}{3}} \right)+$$

$$+\sum_{m=1}^{M}\sum_{n=0}^{N^*(m)}\sum_{i=0}^{I^*(m)}\sum_{l=0}^{L^*(m)} w_{nil}^{j}\left(S_{nil}^{2yd} \frac{\partial (Y_d)_{nil}^{j-1+\frac{2}{3}}}{\partial u^j} \right) p_{nil}^{j-1+\frac{2}{3}} +$$

$$+\sum_{m=1}^{M}\sum_{n=0}^{N^*(m)}\sum_{i=0}^{I^*(m)}\sum_{l=0}^{L^*(m)} w_{nil}^{j}\left(S_{nil}^{2xd} \frac{\partial (X_d)_{nil}^{j-1+\frac{1}{3}}}{\partial u^j} \right) p_{nil}^{j-1+\frac{2}{3}} +$$

$$+\sum_{m=1}^{M}\sum_{n=0}^{N^*(m)}\sum_{i=0}^{I^*(m)}\sum_{l=0}^{L^*(m)} w_{nil}^{j}\left(S_{nil}^{2zd} \frac{\partial (Z_d)_{nil}^{j-1+\frac{1}{3}}}{\partial u^j} \right) p_{nil}^{j-1+\frac{2}{3}} +$$

$$+\sum_{m=1}^{M}\sum_{i=0}^{I^*(m)}\sum_{l=0}^{L^*(m)}\left(w_{N^*(m)il}^{j} \frac{\partial \tilde{X}_{N^*(m)+1,il}^{(j-1)+1/3}}{\partial u^j} p_{N^*(m)il}^{(j-1)+1/3} \right)+$$

$$+\sum_{m=1}^{M}\sum_{i=0}^{I^*(m)}\sum_{l=0}^{L^*(m)}\left(-w_{0il}^{j} \frac{\partial \tilde{X}_{0il}^{(j-1)+1/3}}{\partial u^j} p_{0il}^{(j-1)+1/3} \right)+$$

$$+\sum_{m=1}^{M}\sum_{n=0}^{N^*(m)}\sum_{l=0}^{L^*(m)}\left(w_{nI^*(m)l}^{j} \frac{\partial \tilde{Y}_{n,I^*(m)+1,l}^{(j-1)}}{\partial u^j} p_{nI^*(m)l}^{(j-1)+1/3} \right)+$$

$$+\sum_{m=1}^{M}\sum_{n=0}^{N^*(m)}\sum_{l=0}^{L^*(m)}\left(w_{nI^*(m)l}^{j} \frac{\partial \tilde{Y}_{n,I^*(m)+1,l}^{(j-1)}}{\partial u^j} p_{nI^*(m)l}^{(j-1)+1/3} \right)+$$

$$+\sum_{m=1}^{M}\sum_{n=0}^{N^*(m)}\sum_{i=0}^{I^*(m)}\left(w_{niL^*(m)}^{j} \frac{\partial \tilde{Z}_{ni,L^*(m)+1}^{(j-1)}}{\partial u^j} p_{niL^*(m)}^{(j-1)+1/3} \right)+$$

$$+\sum_{m=1}^{M}\sum_{n=0}^{N^*(m)}\sum_{i=0}^{I^*(m)}\left(w_{niL^*(m)}^{j} \frac{\partial \tilde{Z}_{ni,L^*(m)+1}^{(j-1)}}{\partial u^j} p_{niL^*(m)}^{(j-1)+1/3} \right)+$$

$$+\sum_{m=1}^{M}\sum_{n=0}^{N^*(m)}\sum_{i=0}^{I^*(m)}\sum_{l=0}^{L^*(m)} w_{nil}^{j}\left(S_{nil}^{2xd} \frac{\partial (X_d)_{nil}^{j-1+\frac{1}{3}}}{\partial u^j} \right) p_{nil}^{j-1+\frac{1}{3}} +$$

$$+\sum_{m=1}^{M}\sum_{n=0}^{N^*(m)}\sum_{i=0}^{I^*(m)}\sum_{l=0}^{L^*(m)} w_{nil}^{j}\left(S_{nil}^{2yd} \frac{\partial (Y_d)_{nil}^{j-1}}{\partial u^j} \right) p_{nil}^{j-1+\frac{1}{3}} +$$

$$+\sum_{m=1}^{M}\sum_{n=0}^{N^*(m)}\sum_{i=0}^{I^*(m)}\sum_{l=0}^{L^*(m)} w_{nil}^{j}\left(S_{nil}^{2zd} \frac{\partial (Z_d)_{nil}^{j-1}}{\partial u^j} + \right) p_{nil}^{j-1+\frac{1}{3}}.$$

Since $F(u)$ does not depend explicitly on the control vector $\{u^j\}$, we have $\partial F / \partial u^j = 0$. The derivatives involved in last formula are calculated as described in [11].

Note that the gradient of the cost function calculated using the above formula is exact for the chosen approximation of the optimal control problem.

The problem of optimal control has been solved for various values of the basic parameters of the crystallization process ([7]). One version of the solution of the formulated optimization problem is given below.

The computations were performed for a mold whose cross sections are presented in Fig. 1. Its sizes and other parameters of the problem were given in [13]. The temperature of the furnace walls was set to $1920\,°K$. The coordinate of the required phase boundary varied with time at a constant velocity of 2 mm/min. The initial control was specified as the displacement of the mold at the constant velocity equal to 25 mm/min (Fig. 3). The corresponding cost functional was $I(u_0) = 8.56$. After the optimization the cost functional value decreased by a factor more than 3500 and became equal to $I(u_{opt}(t)) = 0.0024$. The optimal control is shown in Fig. 3. Also, the phase boundary was substantially flattened and at the same time moved at the required speed. Using this control the actual phase boundary nearly coincided with the required one.

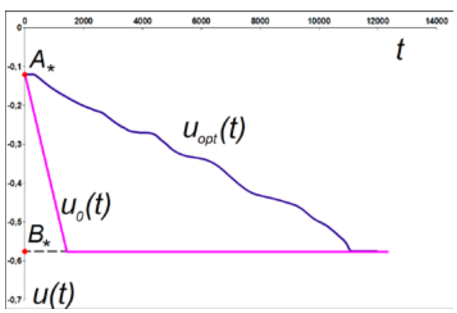

Fig. 3 Displacement of the mold as a function of time

The problem of controlling the phase boundary evolution in the course of solidification of metals with different thermodynamic properties is studied in [14]. The numerical results showed that the actual phase boundary under the found optimal control nearly coincides with the desired one. Thus, we can conclude that the approach proposed in this paper for the control of the phase boundary evolution in solidification is effective and can be applied to materials with various thermodynamic properties.

References

[1] Y. G. Evtushenko, “Computation of Exact Gradients in Distributed Dynamic Systems,” Optimizat. Methods and Software, № 9. pp. 45-75, 1998.

[2] A.F. Albu, “Application of the Fast Automatic Differentiation to Solve Problems of Heat Processes with Phase Transitions,” Doctoral Dissertation in Mathematics and Physics (Dorodnicyn Computing Centre, FRC CSC RAS), 292 p., 2016.

[3] A. F. Albu and V. I. Zubov, “Mathematical Modeling and Study of the Process of Solidification in Metal Casting,” Comput. Math. Math. Phys. Vol. **47**, pp. 843–862, 2007.

[4] A. V. Albu and V. I. Zubov, “Choosing a Cost Functional and a Difference Scheme in the Optimal Control of Metal Solidification,” Comput. Math. Math. Phys. Vol. **51**, pp. 24–38, 2011

[5] A. F. Albu and V. I. Zubov, “Optimal Control of the Solidification Process in Metal Casting,” Comput. Math.Math. Phys. Vol. **48**, pp. 805–815, 2008.

[6] A. F. Albu and V. I. Zubov, “Investigation of the optimal control problem for metal solidification in a new formulation,” Comput. Math. Math. Phys. Vol. **54**, pp. 756–766, 2014.

[7] A. F. Albu and V. I. Zubov, “Investigation of the optimal control of metal solidification for a complex-geometry object in a new formulation,” Comput. Math. Math. Phys. Vol. **54**, pp. 1804–1816, 2014.

[8] A.F. Albu, “Calculation of the thermal radiation in the modeling of the substance crystallization process in the foundry practice,” Informacionnye tekhnologii i vychislitel'nye sistemy, vol.65, № 1, pp.°47-55, 2015.

[9] A. A. Samarskii, “The Theory of Difference Schemes,” (Nauka, Moscow, 1977; Marcel Dekker, New York, 2001).

[10] Ch. Gao, Y. Wang, “A general formulation of Peaceman and Rachford ADI method for the N-dimensional heat diffusion equation,” Int. Comm. Heat Mass Transfer, Vol. 23, No. 6, pp. 845 – 854, 1996.

[11] A. F. Albu, and V. I. Zubov, “Determination of Functional Gradient in an Optimal Control Problem Related to Metal Solidification,” Comput. Math. Math. Phys. Vol.49, pp. 47-70, 2009.

[12] A. V. Albu and V. I. Zubov, “On visual support of the control of dynamical systems,” Optimization and Applications (Vychisl. Tsentr Ross. Akad. Nauk, Moscow, 2010), pp. 33–41.

[13] A. F. Albu and V. I. Zubov, “On the influence of setup parameters on the control of solidification in metal casting,” Comput. Math. Math. Phys. Vol.53, pp. 170–179, 2013.

[14] A. F. Albu, “Control of Phase Boundary Evolution in Metal Solidification for New Thermodynamic Parameters of the Metal,” Comput. Math. Math. Phys. Vol.56, pp. 756–763, 2016.